0026-895X/95/050869-11$3.00/0

MOLECULAR PHARMACOLOGY, 48:869–879 (1995).

Molecular Cloning and Expression of Multiple Isoforms of Human Prostaglandin E Receptor EP_3 Subtype Generated by Alternative Messenger RNA Splicing: Multiple Second Messenger Systems and Tissue-Specific Distributions

MASATO KOTANI, ISSEI TANAKA, YOSHIHIRO OGAWA, TAKESHI USUI, KIYOSHI MORI, ATSUSHI ICHIKAWA, SHUH NARUMIYA, TERUYA YOSHIMI, and KAZUWA NAKAO

Second Division, Department of Medicine (M.K., I.T., Y.O., T.U., K.M., K.N.), and Department of Pharmacology (S.N.), Faculty of Medicine, and Department of Physiological Chemistry (A.I.), Faculty of Pharmaceutical Sciences, Kyoto University, Kyoto, and Second Department of Internal Medicine, Hamamatsu University, School of Medicine, Hamamatsu (M.K., T.Y.), Japan

Received February 20, 1995; Accepted August 21, 1995

SUMMARY

Five distinct cDNA clones encoding four different isoforms of human prostaglandin (PG) E receptor EP_3 subtype were isolated from a human kidney cDNA library. Two cDNA clones differed only in their 3′-untranslated regions. The four isoforms, tentatively named $EP_{3\text{-I}}$, $EP_{3\text{-II}}$, $EP_{3\text{-III}}$, and $EP_{3\text{-IV}}$, which were generated by alternative mRNA splicing, had identical amino acid sequences except for their different carboxyl-terminal tails. Transfection experiments revealed that all the four isoforms show high binding affinities to PGE_2, PGE_1, and M&B28767, an EP_3-specific agonist, whereas their downstream signaling pathways are divergent. M&B28767 increased cAMP concentrations in cells expressing $EP_{3\text{-II}}$ and $EP_{3\text{-IV}}$, whereas it inhibited forskolin-induced cAMP accumulations in cells expressing all EP_3 isoforms. M&B28767 also stimulated phosphoinositide turnover in cells expressing $EP_{3\text{-I}}$ and $EP_{3\text{-II}}$. Northern blot analysis revealed that the EP_3 gene is expressed in a wide variety of human tissues. The human EP_3 mRNA was present most abundantly in the kidney, pancreas, and uterus. A substantial expression was also detected in the heart, liver, skeletal muscle, small intestine, colon, prostate, ovary, and testis. Furthermore, reverse transcription-polymerase chain reaction analysis demonstrated tissue-specific expressions of the five different EP_3 mRNA species. The present study suggests the presence of the multiple systems of PGE_2/EP_3 isoforms and leads to the better understanding of its physiological and pathophysiological implications in humans.

The prostaglandins are oxygenated metabolites of arachidonic acid and exert various physiological functions as local mediators in the body (1). Among them, PGE_2 has a wide variety of biological actions that include contraction and relaxation of smooth muscle, modulation of neurotransmitter release, inhibition of gastric acid secretion, and inhibition of water reabsorption in renal collecting tubules (2). These actions of PGE_2 are believed to be mediated by multiple receptors that elicit cellular responses by activating G proteins. PGE receptors have been pharmacologically classified into at least four subtypes: EP_1, EP_2, EP_3, and EP_4 (2, 3).

We have succeeded in the isolation of mouse EP_1, EP_3, and EP_4 and bovine EP_3 subtype cDNAs (4–7) and demonstrated that they belong to the G protein-coupled receptor superfamily with seven transmembrane domains. The cDNA sequence of human EP_2 subtype has been recently reported by Regan *et al.* (8). Our subsequent studies revealed that previously designated "EP_2" subtype is sensitive to AH23848, a specific antagonist of EP_4, and insensitive to butaprost, a specific agonist of EP_2 (8a). Therefore, in the present report, we call the "EP_2" subtype originally cloned by Honda *et al.* and Bastien *et al.* (5, 9) "EP_4."

Of particular notice is the presence of multiple EP_3 isoforms, i.e., mouse $EP_{3\alpha}$, $EP_{3\beta}$, and $EP_{3\gamma}$ and bovine EP_{3A}, EP_{3B}, EP_{3C}, and EP_{3D}, which differ only in their carboxyl-terminal tails (7, 10, 11). Furthermore, rabbit and rat EP_3 subtypes also have multiple isoforms with divergent carboxyl-terminal tails (12, 13). These isoforms are believed to be generated by alternative mRNA splicing. We previously demonstrated that mouse $EP_{3\alpha}$ and $EP_{3\beta}$ show different agonist-induced desensitization in coupling to G_i protein (14) and

This work was supported by research grants from the Japanese Ministry of Education, Science and Culture and a research grant from ONO Medical Research Foundation.

ABBREVIATIONS: bp, basepair(s); kb, kilobase(s); MES, 4-morpholineethanesulfoic acid; PG, prostaglandin; RT-PCR, reverse transcription-polymerase chain reaction; SSC, standard saline citrate; IP_3, inositol 1,4,5-trisphosphate; CHO, Chinese hamster ovary; SDS, sodium dedocyl sulfate; M&B28767, .

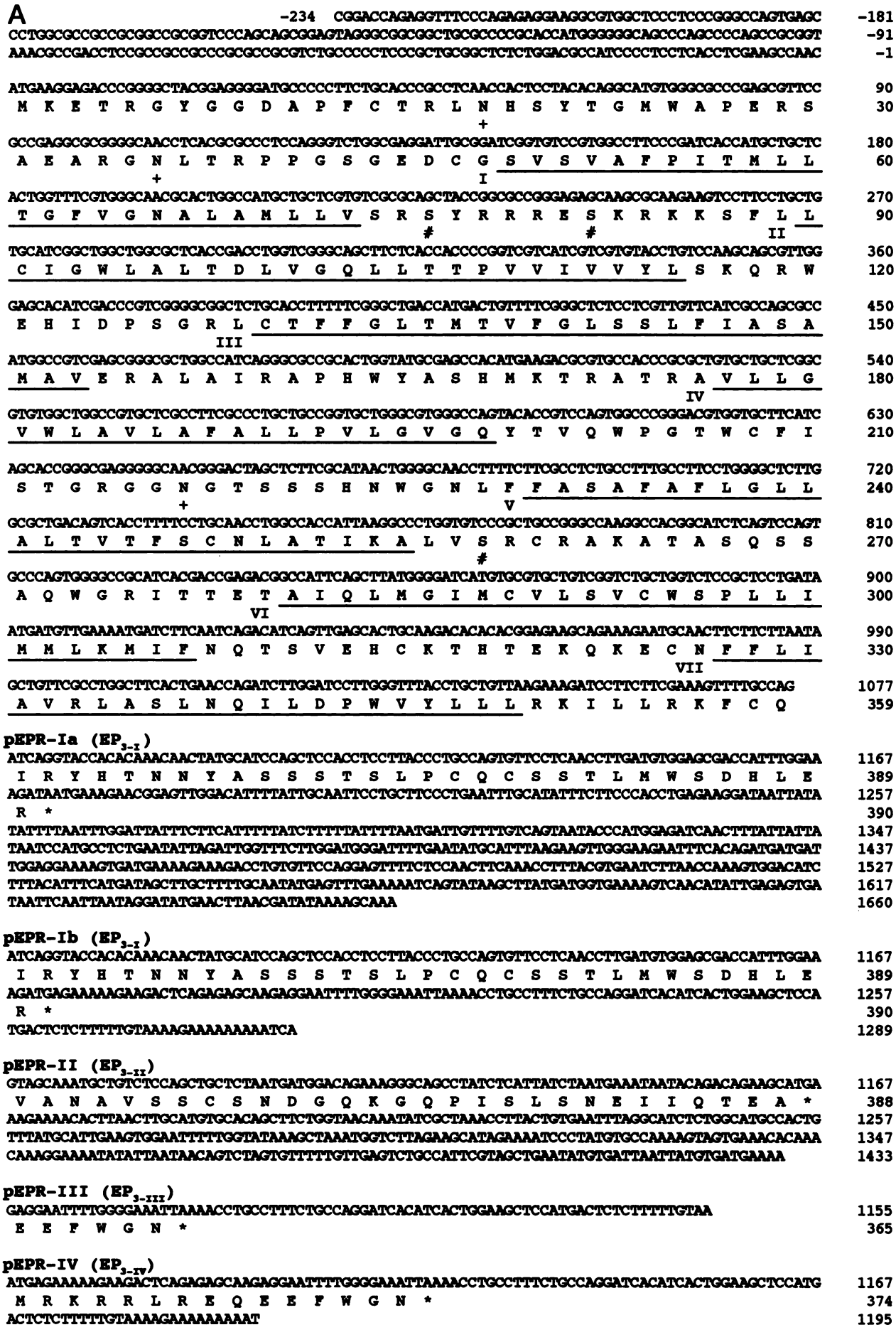

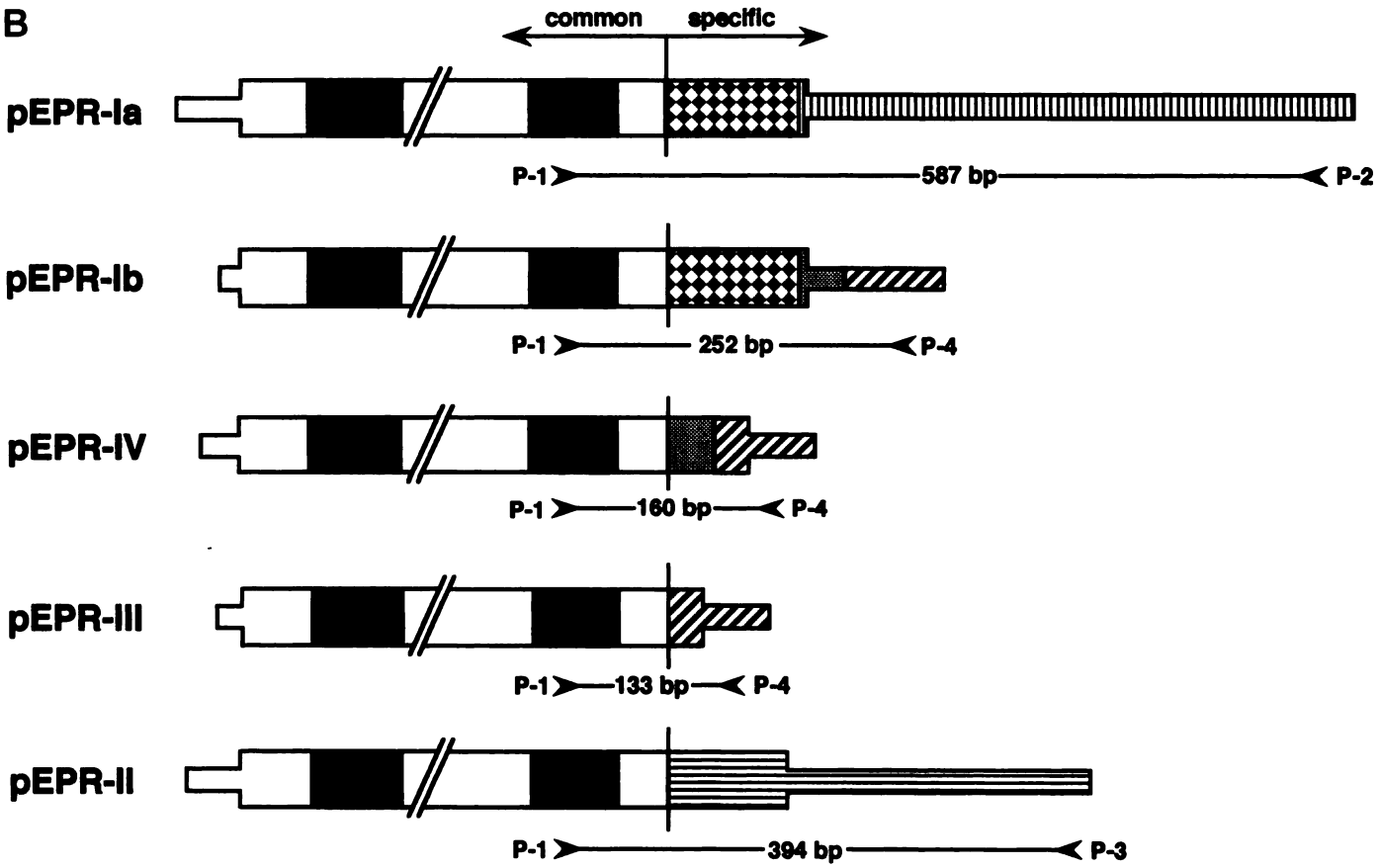

Fig. 1. Comparison of nucleotide and deduced amino acid sequences and cDNA structures of pEPR-Ia, -Ib, -II, -III, and -IV and positions of PCR primers for RT-PCR. A (*opposite*), Nucleotide sequences are shown in smaller letters, and deduced amino acid sequences are shown in larger letters. Nucleotides are numbered with +1, referring to the first nucleotide of the methionine initiation codon. The putative transmembrane domains (I through VII) are *underlined*. *, Potential *N*-glycosylation sites. #, Potential protein kinase C phosphorylation sites. The 5′ untranslated nucleotide sequence is of p-EPR-Ia containing the furthest nucleotide sequence upstream from the initiation codon among the representative five cDNA clones. B (*above*), Representation of pEPR-Ia, -Ib, -II, -III, and -IV and positions of PCR primers used for RT-PCR analyses in Fig. 9. *Wide areas*, coding region of each clone. *Narrow areas*, 5′ and 3′ noncoding regions. *Open and filled areas*, nucleotide sequences of the five cDNAs from the 5′-untranslated regions to the 1077th guanine nucleotide. Filled areas, putative transmembrane domain regions. *Checkered, shaded, and diagonal striped areas*, regions of pEPR-Ib: positions +1078 to +1169, +1170 to +1196, and +1197 to +1274, respectively. *Vertical and horizontal striped areas*, regions of pEPR-Ia (position +1078 to +1660) and pEPR-II (position +1078 to +1433), respectively. *Arrows*, positions of PCR primers and expected sizes of PCR products.

that mouse $EP_{3\gamma}$ is coupled not only to G_i protein but also to G_s (11), suggesting that different carboxyl-terminal tails are involved in different second messenger systems. We also demonstrated that carboxyl-terminal tails of four bovine EP_3 isoforms determined their second messenger systems (7). Very recently, three isoforms of human EP_3 subtype have been isolated (15–18). (During the preparation of this manuscript, Adam *et al.* (15) and Regan *et al.* (16) reported the isolation of three human EP_3 isoforms, $EP_{3\text{-I}}$, $EP_{3\text{-II}}$, and $EP_{3\text{-III}}$ (15), and the latter group demonstrated that these isoforms have inhibitory effects on adenylate cyclase pathway (16), whereas other possible second messenger systems of EP_3 isoforms have been unknown.)

In the present study, we isolated five distinct cDNA clones encoding four different EP_3 isoforms, designated $EP_{3\text{-I}}$, $EP_{3\text{-II}}$, $EP_{3\text{-III}}$, and $EP_{3\text{-IV}}$, which are generated by alternative mRNA splicing. $EP_{3\text{-I}}$, $EP_{3\text{-II}}$, and $EP_{3\text{-III}}$ correspond to those reported by Adam *et al.*; however, $EP_{3\text{-IV}}$ was a novel isoform. Transfection experiments showed that the four EP_3 isoforms were coupled to multiple second messenger systems, stimulation and/or inhibition of adenylate cyclase pathway, and/or stimulation of phosphoinositide turnover. Furthermore, to elucidate the tissue distribution of EP_3 isoforms in humans, we performed Northern blot and RT-PCR analyses. The present study will help elucidate the functions of PGE_2 and EP_3 isoforms in humans.

Materials and Methods

Molecular cloning. Approximately 3.0×10^5 plaques from a human kidney λgt10 cDNA library (Clontech Laboratories, Palo Alto, CA) were transferred onto nitrocellulose membranes (Schleicher & Schuell, Keene, NH) and screened with the ^{32}P-labeled *Eco*RI/*Hind*III mouse $EP_{3\alpha}$ cDNA fragment as a probe (6). Prehybridization and hybridization were performed as described (19) in 5× SSC containing 25% formamide, 1× Denhardt's solution, 0.1% SDS, and 100 μg/ml salmon sperm DNA at 37°. The membranes were washed in 2× SSC, 0.1% SDS at 37°. Eighteen positive phage clones were isolated, and their DNAs were purified by the plate lysate

method (20). Inserts of 1.0–1.9 kb were subcloned into the *Eco*RI site of pBluescript KS(−) vector (Stratagene, La Jolla, CA), which were sequenced using DyeDeoxy Terminator Cycle Sequencing Kit (Applied Biosystems, Foster City, CA). These plasmid clones were classified into five groups based on their nucleotide sequences and restriction maps, and the representative clones were designated as pEPR-Ia, pEPR-Ib, pEPR-II, pEPR-III, and pEPR-IV (Fig. 1).

Genomic Southern blot analysis. Approximately 10 μg of human genomic DNA isolated from blood leukocytes was digested with restriction enzymes *Eco*RI, *Hind*III, *Bam*HI, and *Bgl*II; electrophoresed on a 0.7% agarose gel; and transferred onto a Biodyne A nylon membrane (Pall, Glen Cove, NY) (20). Southern blot analysis was performed as described previously (21) using the ^{32}P-labeled *Eco*RI/*Bgl*II fragment of pEPR-Ia (position −234 to +1016 in Fig. 1A) as a probe.

Plasmid constructions and transfection experiments. The *Hind*III/*Xba*I fragments of pEPR-Ia, pEPR-II, pEPR-III, and pEPR-IV were subcloned into a eukaryotic expression vector, pRc/RSV (Invitrogen, San Diego, CA) and were designated as pRc-pEPR-I, pRc-pEPR-II, pRc-pEPR-III, and pRc-pEPR-IV, respectively. These plasmids or pRc/RSV alone (mock-transfected as a control) were transfected transiently into COS-7 cells or CHO cells by the DEAE-dextran method (22).

Construction of stable CHO cell line. The CHO cells transfected with pRc-pEPR-I, pRc-pEPR-II, pRc-pEPR-III, or pRc-pEPR-IV were cultured for 72 hr in Ham's F-12 medium (ICN Biomedicals, Tokyo, Japan). Then, CHO cells were reseeded and cultured in Ham's F-12 containing 800 μg/ml of the antibiotic G418 (GIBCO-BRL, Grand Island, NY) (23). A CHO cell line was isolated by a colony, and the expressions of transfected cDNA in several cell lines were assessed by their specific [^{3}H]PGE_2 binding.

Crude membrane preparation and ligand binding assay. Seventy-two hours after transfection with pRc-pEPR-Ia, -II, -III, or -IV, COS-7 cells were harvested, and crude membranes were prepared as described previously (19). The crude membranes of stable CHO cells were prepared by the same method. For saturation experiments, 40 μg of crude membrane protein was incubated with 1–32 nM of [5,6,8,11,12,14,15-^{3}H]PGE_2 (154 Ci/mmol) (Du Pont-New England Nuclear, Boston, MA) in 100 μl of a solution containing 20 mM MES/NaOH (pH6.0), 10 mM $MgCl_2$, and 1 mM EDTA at 30° for 1 hr. For displacement experiments, 40 μg of membrane protein was incubated with 4 nM of [^{3}H]PGE_2 and unlabeled PGE_1, PGE_2, and $PGF_{2\alpha}$ (Nacalai Tesque, Kyoto, Japan), PGD_2 (Sigma Chemical Co., St. Louis, MO), or the EP_3 receptor agonist M&B28767 (a generous gift from Dr. M. P. L. Caton, Rhone-Poulenc Ltd.) (19). The incubation mixture was filtered through a GF/C filter (Whatman International Ltd., Maidstone, UK), and bound radioactivity was determined with a liquid scintillation counter.

cAMP measurements. COS-7 cells at 24 hr after transfection or stable CHO cells were plated into 24-well plates (1×10^5 cells/well) and cultured at 37° for 24 hr. Cells were washed with phosphate-buffered saline and incubated in 500 μl of Dulbecco's modified Eagle's medium (Biomedicals, Tokyo, Japan) or in Ham's F-12 containing 0.1% bovine serum albumin and 1 mM of 3-isobutyl-1-methylxanthine (Nacalai Tesque) at 37° for 10 min. Then, various concentrations of M&B28767 (see Figs. 4 and 5) and 1 μM of forskolin or vehicle were added, and cells were incubated for 30 min at 37°. The reactions were terminated by the addition of an equal volume of 12% trichloroacetic acid. The cAMP levels were measured with a commercially available radioimmunoassay kit (Yamasa Corp., Tokyo, Japan) (24).

IP_3 measurements. COS-7 cells at 48 hr after transfection or stable CHO cells were scraped off from the plates and suspended in Dulbecco's modified Eagle's medium or Ham's F-12. COS-7 cells were stimulated with the vehicle or 1 μM of M&B28767 for 30 sec at 37°. CHO cells were stimulated with the vehicle or 100 pM, 10 nM, and 1 μM of M&B28767. The IP_3 levels were measured with a radioreceptor assay kit (New England Nuclear) (25).

Total RNA extraction and poly(A)$^+$ RNA purification. Human tissues were obtained at autopsy, and tRNA was extracted by the guanidinium thiocyanate/cesium chloride method (20). Poly(A)$^+$ RNA was isolated with the use of a biotinylated oligo(dT) primer (Poly A Tract, Promega Corp., Madison, WI). The present study was conducted with informed consent and approved by the Ethical Committee on Human Research of Kyoto University (No. 61–98).

Northern Blot analysis. Northern blot analysis were performed with the Human MTN Blot (Clontech) or blots with 2 μg each of poly(A)$^+$ RNA extracted from the human uterus, adrenal, and thyroid. These blots were hybridized with the ^{32}P-labeled *Eco*RI/*Bgl*II pEPR-Ia cDNA fragment as a probe.

RT-PCR. To examine differential expressions of the five EP_3 subtype mRNA species in human tissues, RT-PCR analyses were performed. Two hundred nanograms of tRNA extracted from the human tissues were reverse-transcribed with the use of an oligo(dT) primer (SuperScript II, GIBCO-BRL). The positions of four primers for RT-PCR are shown in Fig. 1B: sense primer common to all the isoforms, P-1 (position +1009 to +1028); antisense primers for cDNA tail, P-2 (position +1576 to +1595) for pEPR-Ia; P-3 (position +1383 to +1402) for pEPR-II; and P-4 (position +1241 to +1260) for pEPR-Ib, pEPR-III and pEPR-IV, as described. The reaction profile was as follows: denaturation at 94° for 30 sec, annealing at 55° for 30 sec, and extension at 72° for 60 sec, for 35 cycles. The RT-PCR for human β-actin was also performed with a sense primer, 5′-ATCATGTTTGAGACCTTCAACACCCC-3′, and an antisense primer, 5′-CTTGATCTTCATTGTGCTGGGTGCCA-3′ (26), and was used as an internal control. Five microliters of the reaction mixture were loaded on a 3% agarose gel (NuSieve 3:1 Agarose, FMC BioProducts, Rockland, ME) and transferred onto a nylon membrane. The membrane was hybridized with a ^{32}P-end-labeled internal oligo DNA probe (position +1038 to +1057) or a ^{32}P-labeled human β-actin genomic DNA fragment (Wako Pure Chemical, Osaka, Japan) (25) in a solution containing 6× SSC, 0.1% SDS, and 100 μg/ml salmon sperm DNA at 37°. The membrane was washed in 6× SSC, 0.1% SDS at 50° and exposed to a film with intensifiers for 6 hr.

Statistical analysis. Statistical analyses were performed with analysis of variance, and a value of $p < 0.05$ was considered statistically significant.

Results

Molecular cloning. Approximately 3×10^5 recombinants were screened, and 18 clones were obtained, 12 of which contained the entire coding sequences in the inserts of 1.3–1.9 kb. These clones were classified into five groups according to their nucleotide sequences and restriction mappings. The representative clones were designated as pEPR-Ia, pEPR-Ib, pEPR-II, pEPR-III, and pEPR-IV (Fig. 1).[1]

Nucleotide sequence analysis. Fig. 1A shows the nucleotide and deduced amino acid sequences of the five representative cDNA clones (pEPR-Ia, pEPR-Ib, pEPR-II, pEPR-III, and pEPR-IV), and their structures are schematically illustrated in Fig. 1B. The common initiation codon of the five clones was proceeded by in-frame termination codons, and the surrounding nucleotide sequences agreed well with the consensus sequences (27). pEPR-Ia, -Ib, -II, -III, and -IV contained open reading frames of 1170, 1170, 1164, 1095, and 1122 bp, respectively. All the clones shared the common nucleotide sequences from the 5′- untranslated portions up to the 1077th guanine nucleotide (Fig. 1B, *open and closed areas*) but differed further downstream in the 3′ tail portions.

[1] The nucleotide sequences reported in this article have been submitted to the GenBank/EMBL Data Bank with accession numbers D38297 through D38301.

pEPR-Ia and pEPR-Ib had identical open reading frames and differed only in their 3′- untranslated regions. pEPR-IV was identical to pEPR-Ib except for a deletion of a 92-bp nucleotide sequence (Fig. 1B, *checkered area*), which resulted in a frame shift to give rise to another open reading frame of 45 bp in pEPR-IV. pEPR-III was shorter than pEPR-IV by 27 bp (Fig. 1B, *shaded area*), with no frame shift. Downstream of the 5′ common nucleotide sequence, pEPR-II was unrelated to other clones and contained a unique nucleotide sequence (Fig. 1B, *horizontal striped area*).

Amino acid sequence analysis. pEPR-Ia, -Ib, -II, -III, and -IV encoded 390, 390, 388, 365, and 374 amino acid proteins, respectively. Among them, pEPR-Ia and pEPR-Ib encoded identical amino acid sequences. The five distinct cDNA clones therefore encoded four different amino acid sequences, all of which shared the common 359-amino acid sequence up to Glu-359 residue (Fig. 1A) and differed further downstream in the carboxyl-terminal tails. The hydropathicity profile determined by the Kyte and Doolittle method (28) reveals that all the cDNA clones have seven hydrophobic segments in the 5′ common sequences, which suggests that the five cDNA clones all encode human EP_3 isoforms in the G protein-coupled receptor superfamily. Thus, we isolated five distinct cDNA clones encoding four different human EP_3 isoforms and designated the receptor encoded by pEPR-Ia and pEPR-Ib as $EP_{3\text{-I}}$, the receptor encoded by pEPR-II as $EP_{3\text{-II}}$, the receptor encoded by pEPR-III as $EP_{3\text{-III}}$, and the receptor encoded by pEPR-IV as $EP_{3\text{-IV}}$, respectively. Downstream of the common 359-amino acid sequence, $EP_{3\text{-I}}$ contained a 31-amino acid sequence, which was replaced by another 15-amino acid sequence in $EP_{3\text{-IV}}$. $EP_{3\text{-III}}$ had an identical amino acid sequence with $EP_{3\text{-IV}}$ except for a deletion of 9 amino acid residues, which was encoded by the 27-bp nucleotide sequence in $EP_{3\text{-IV}}$. $EP_{3\text{-II}}$ had a unique amino acid sequence downstream of the common 359-amino acid sequence. These EP_3 isoforms have three potential *N*-glycosylation sites (Asn-18, Asn-36, and Asn-217) and three potential protein kinase C phosphorylation sites (Ser-76,Ser-82, and Ser-258) in the common 359-amino acid sequences (29).

The homologies in the amino acid sequences between the common amino acid sequence of the four human EP_3 isoforms and those of mouse EP_3 and bovine EP_3 isoforms were 80.8% and 85.8%, respectively. The homologies between the four EP_3 isoforms and other human prostanoid receptors (EP_1, EP_2, EP_4, IP, TP, and FP) were <60% at the amino acid level (8, 9, 30–33). The amino acid sequences of $EP_{3\text{-I}}$, $EP_{3\text{-II}}$, and $EP_{3\text{-III}}$ revealed in the present study were identical to those of three human EP_3 isoforms, which Adam *et al.* (15) and Regan *et al.* (16) have recently reported. In contrast, $EP_{3\text{-IV}}$ was a novel isoform, being unique in the insertion of extra 9 amino acid residues in the carboxyl-terminal tail of $EP_{3\text{-III}}$. Homologues of $EP_{3\text{-IV}}$ have never been reported in any other species.

Genomic Southern blot analysis. Southern blot analysis of human genomic DNA using the ^{32}P-labeled *Eco*RI/*Bgl*II fragment of pEPR-Ia (position −234 to +1016 in Fig. 1A) identified a single hybridizing band on digestion with restriction enzymes *Eco*RI, *Hind*III, *Bgl*II, and *Bam*HI (5.8, 6.9, 6.2, and 3.5 kb, respectively) (Fig. 2).

Ligand binding assays. To confirm that the cDNA clones isolated in the present study encode receptors specific for

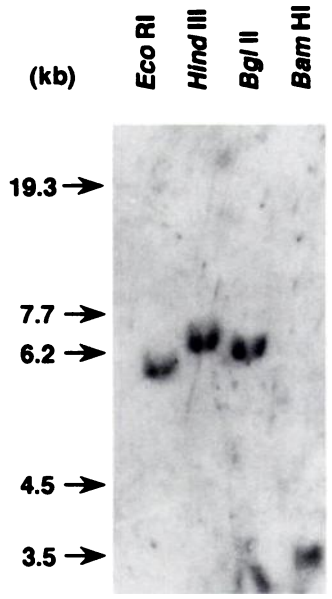

Fig. 2. Human genomic Southern blot analysis. Samples of human genomic DNA (approximately 10 μg/lane) digested with restriction enzymes *Eco*RI, *Hind*III, *Bgl*II, and *Bam*HI were analyzed by 0.7% agarose gel electrophoresis, blotted, and hybridized with the ^{32}P-labeled *Eco*RI/*Bgl*II cDNA fragment of pEPR-Ia. The *Eco*T14I fragments of lDNA are used as size markers.

PGE, we performed saturation and displacement experiments of the transiently expressed receptors in COS-7 cells and CHO cells, which stably express $EP_{3\text{-IV}}$. [^{3}H]PGE_2 specifically bound to the crude membranes prepared from cells expressing $EP_{3\text{-I}}$, $EP_{3\text{-II}}$, $EP_{3\text{-III}}$, or $EP_{3\text{-IV}}$. With the crude membranes prepared from $EP_{3\text{-I}}$-, $EP_{3\text{-II}}$-, and $EP_{3\text{-III}}$-expressing cells, specific [^{3}H]PGE_2 bindings were displaced by unlabeled PGE_2, PGE_1, and M&B28767 (data not shown), which was consistent with previous reports (15). Table 1 shows the K_i values for PGE_2, PGE_1, and M&B28767 against $EP_{3\text{-I}}$, $EP_{3\text{-II}}$, $EP_{3\text{-III}}$, and $EP_{3\text{-IV}}$. Fig. 3 shows the result of displacement experiments with various prostaglandins and M&B28767, saturation plot, and Scatchard analysis for $EP_{3\text{-IV}}$ isoform using COS-7 cell membranes (Fig. 3, A through C) or CHO cell membranes (Fig. 3A). As shown in Fig. 3A, PGE_2 and PGE_1 were almost equipotent in inhibiting specific [^{3}H]PGE_2 binding. $PGF_{2\alpha}$ showed lower affinity by approximately 2 orders of magnitude than PGE_2 and PGE_1 in inhibiting specific [^{3}H]PGE_2 binding. PGD_2 showed the lowest affinity among prostaglandins examined. M&B28767 showed higher affinity than PGE_2. The rank order was M&B28767 > PGE_2 ≥ PGE_1 ≫ $PGF_{2\alpha}$ ≥ PGD_2. The binding characteristics of $EP_{3\text{-IV}}$ were well consistent with those of $EP_{3\text{-I}}$, $EP_{3\text{-II}}$, and $EP_{3\text{-III}}$ (15) and with those of mouse PGE receptor EP_3 subtype (6). Scatchard analysis for

TABLE 1

Competition for [^{3}H]PGE_2 specific binding to membranes of COS-7 cells transfected with pRc-pEPR-Ia, -II, -III, and -IV

Competing ligand	K_i			
	$EP_{3\text{-I}}$	$EP_{3\text{-II}}$	$EP_{3\text{-III}}$	$EP_{3\text{-IV}}$
	n			
PGE_2	1.2	1.6	1.3	1.7
PGE_1	3.8	3.9	2.6	5.5
M&B28767	0.9	0.6	0.4	0.4

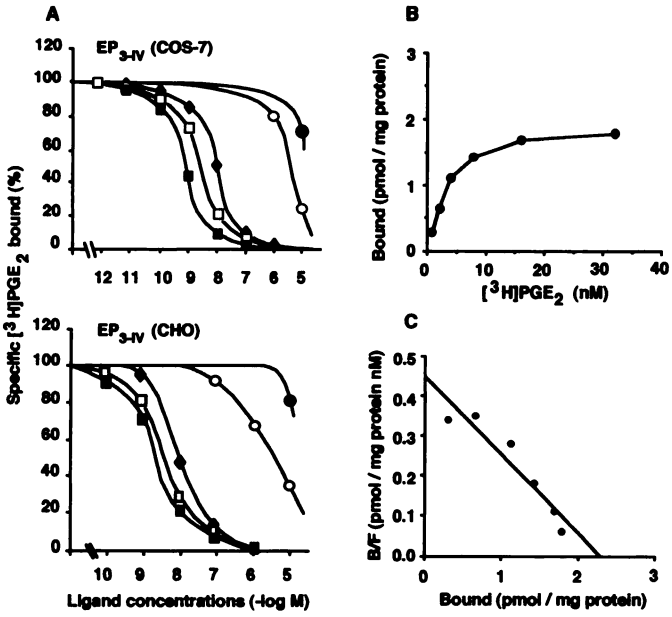

Fig. 3. Competition for $[^3H]PGE_2$ specific binding, saturation plot, and Scatchard analysis of pEPR-IV-transfected COS-7 cell and CHO cell membranes. A, Displacement of $[^3H]PGE_2$ binding by various prostaglandins and M&B28767 with COS-7 cell membranes (*top*) or CHO cell membranes (*top*). Unlabeled prostaglandins and M&B28767 were added to the binding assay mixture at indicated concentrations, and $[^3H]PGE_2$ binding was determined as described in Materials and Methods. The prostaglandins used were PGE_2 (□), PGE_1 (♦), PGD_2, (●), $PGF_{2\alpha}$ (○), and M&B28767 (■). B and C, Saturation plot and Scatchard analysis of pRc-pEPR-IV transfected COS-7 cell membranes, respectively.

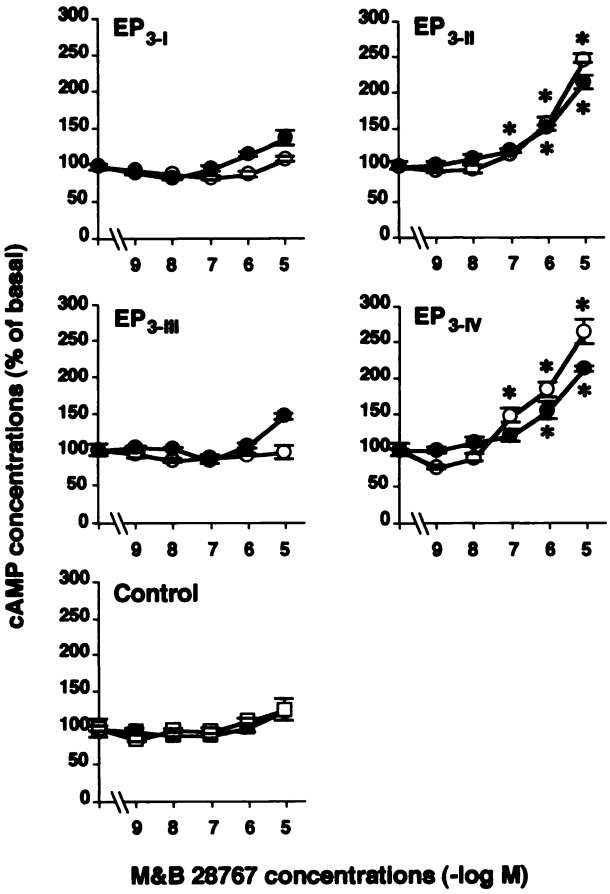

Fig. 4. Comparison of the effect of M&B28767 on the cAMP level in COS-7 cells and CHO cells expressing EP_3 isoforms. COS-7 cells (●) or CHO cells (○) expressing EP_3 isoforms, mock-transfected COS-7 cells (■), and untransfected CHO cells (□) were incubated at 37° for 30 min with the vehicle or M&B28767 at the indicated concentrations. Then, cAMP formation was determined as described in Materials and Methods. Each point represents the mean ± standard error of two sets of triplicated determinations in COS-7 cells or the mean ± standard error of one set of quadruplicated determinations in CHO cells. The cAMP concentrations in COS-7 cells expressing $EP_{3\text{-I}}$, $EP_{3\text{-II}}$, $EP_{3\text{-III}}$, and $EP_{3\text{-IV}}$ and in mock-transfected COS-7 cells without M&B28767 amounted to 1.38 ± 0.03, 1.44 ± 0.05, 1.90 ± 0.06, 1.52 ± 0.04, and 1.50 ± 0.05 pmol/10^5 cells, respectively, and the cAMP concentrations in CHO cells expressing $EP_{3\text{-I}}$, $EP_{3\text{-II}}$, $EP_{3\text{-III}}$, and $EP_{3\text{-IV}}$ and in untransfected CHO cells without M&B28767 amounted to 1.20 ± 0.05, 1.42 ± 0.08, 1.05 ± 0.05, 1.25 ± 0.04, and 0.95 ± 0.02 pmol/10^5 cells, respectively. *, Significant increases in cAMP levels compared with mock-transfected cells incubated with the same concentrations of M&B28767 ($p < 0.05$).

a novel isoform $EP_{3\text{-IV}}$ revealed that the dissociation constant value is 5.0 nM and that the maximal specific $[^3H]PGE_2$ binding is 2.24 pmol/mg protein using COS-7 cell membranes (Fig. 3, B and C). As shown in Fig. 3A, the binding characteristics of $EP_{3\text{-IV}}$ with the stable cell line were consistent with those of COS-7 cells transiently expressing $EP_{3\text{-IV}}$. In the CHO cells stably expressing $EP_{3\text{-IV}}$, the maximal specific $[^3H]PGE_2$ binding was 4.16 pmol/mg protein. The B_{max} values of COS-7 cells transiently expressing $EP_{3\text{-I}}$, $EP_{3\text{-II}}$, $EP_{3\text{-III}}$, and $EP_{3\text{-IV}}$ were 4.5, 4.6, 5.7, and 3.6 fmol/10^6 cells, respectively, and those of CHO cells stably expressing $EP_{3\text{-I}}$, $EP_{3\text{-II}}$, $EP_{3\text{-III}}$, and $EP_{3\text{-IV}}$ were 10.2, 8.7, 12.1, and 12.3 fmol/10^6 cells, respectively.

cAMP Measurement. To examine the second messenger systems of EP_3 isoforms, we used COS-7 cells transiently expressing EP_3 isoforms. Furthermore, to confirm the results with COS-7 cells, we repeated these experiments using CHO cells stably expressing EP_3 isoforms. We compared agonist-induced cAMP accumulations between mock-transfected COS-7 cells and cells expressing $EP_{3\text{-I}}$, $EP_{3\text{-II}}$, $EP_{3\text{-III}}$, or $EP_{3\text{-IV}}$ (Fig. 4) and repeated these experiments with CHO cells stably expressing $EP_{3\text{-I}}$, $EP_{3\text{-II}}$, $EP_{3\text{-III}}$, and $EP_{3\text{-IV}}$ (Fig. 4). In mock-transfected COS-7 cells, up to 1 μM M&B28767 did not increase basal cAMP levels compared with unstimulated condition, although as much as 10 μM M&B28767 increased the cAMP level by ~24% (Fig. 4). The cAMP levels were unchanged in cells expressing either $EP_{3\text{-I}}$ or $EP_{3\text{-III}}$ compared with mock-transfected cells (Fig. 4). In contrast, M&B28767 significantly increased the cAMP levels in cells expressing $EP_{3\text{-II}}$ compared with mock-transfected cells in a concentration-dependent manner within the range from 100 nM to 10 μM. Similarly, the cAMP level was increased significantly in cells expressing $EP_{3\text{-IV}}$ when >1 μM M&B28767 was added, and it reached a ~1.7-fold higher level than in mock-transfected cells at 10 μM. In CHO cells expressing $EP_{3\text{-I}}$ or $EP_{3\text{-III}}$, cAMP levels were not changed compared with untransfected CHO cells (Fig. 4). In CHO cells expressing $EP_{3\text{-II}}$, cAMP levels were significantly increased within the range of 1 μM to 10 μM compared with those of untransfected cells. In CHO cells expressing $EP_{3\text{-IV}}$, the cAMP levels were also significantly increased when >100 nM of M&B28767 was added. We also examined the effects of M&B28767 on forskolin-induced cAMP accumulation in cells expressing $EP_{3\text{-I}}$, $EP_{3\text{-II}}$, $EP_{3\text{-III}}$, or $EP_{3\text{-IV}}$. As reported re-

cently (16), forskolin-induced cAMP accumulation was suppressed in COS-7 cells and CHO cells expressing $EP_{3\text{-I}}$, $EP_{3\text{-II}}$, and $EP_{3\text{-III}}$ (data not shown). As shown in Fig. 5, the cAMP concentrations of COS-7 cells expressing $EP_{3\text{-IV}}$ were significantly decreased within the range of from 1 nM to 100 nM of M&B28767 compared with those of COS-7 cells stimulated by forskolin alone (Fig. 5). As shown in Fig. 5, in CHO cells stably expressing $EP_{3\text{-IV}}$, the cAMP concentrations were significantly decreased in a dose-dependent fashion when >10 pM of M&B 28767 was added and decreased to 38% of those of cells stimulated by forskolin alone (Fig. 5).

IP_3 measurement. To examine EP_3 isoform-mediated changes in phosphoinositide turnover, IP_3 concentrations were determined in COS-7 cells expressing $EP_{3\text{-I}}$, $EP_{3\text{-II}}$, $EP_{3\text{-III}}$, or $EP_{3\text{-IV}}$ and in mock-transfected cells with or without 1 μM M&B28767 (Fig. 6). Furthermore, in CHO cell lines, IP_3 concentrations were measured with or without 100 pM, 10 nM, and 1 μM of M&B28767 (Fig. 6). M&B28767 induced a ~55% and ~45% increase in IP_3 level in COS-7 cells expressing $EP_{3\text{-I}}$ and $EP_{3\text{-II}}$, respectively, whereas no significant changes were observed in cells expressing $EP_{3\text{-III}}$ or $EP_{3\text{-IV}}$ or in mock-transfected cells (Fig. 6). In CHO cells expressing $EP_{3\text{-I}}$ and $EP_{3\text{-II}}$, IP_3 concentrations were increased in a concentration-dependent manner when >10 nM of M&B28767 was added and reached ~296% and ~180% of concentrations of unstimulated cells at 1 μM, respectively (Fig. 6).

Northern blot analysis. Northern blot analysis identified five distinct hybridizing mRNA species in a wide variety of human tissues (Fig. 7). The sizes of the bands were ~7.5, 5.0, 4.5, 2.5, and 1.9 kb, respectively. The 4.5-kb mRNA was expressed most widely in human tissues examined. Two mRNA species of 2.5 and 1.9 kb were also widely expressed with largely overlapping distributions. In contrast, the 7.5-kb mRNA species showed a sparse distribution, and the 5.0-kb mRNA species was detected only in the kidney. These results revealed tissue-specific distributions of the five EP_3 mRNA species. As a whole, the human EP_3 receptor gene was expressed abundantly in the kidney, pancreas, and uterus. A substantial expression was also observed in the heart, liver, skeletal muscle, testis, ovary, small intestine, and colon. Little but significant expression was observed in the placenta, lung, thymus, prostate, thyroid, and adrenal.

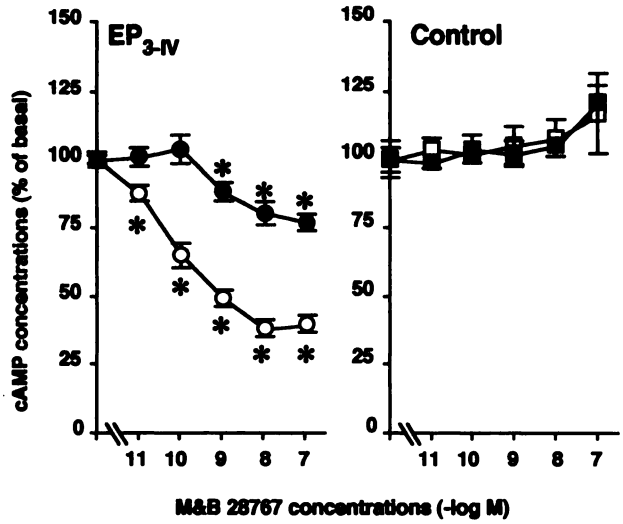

Fig. 5. Inhibition of forskolin-induced cAMP accumulation in COS-7 cells and CHO cells expressing $EP_{3\text{-IV}}$ by M&B28767. COS-7 cells (●) or CHO cells (○) expressing $EP_{3\text{-IV}}$ isoform, mock-transfected COS-7 cells (■), and untransfected CHO cells (□) were incubated at 37° for 30 min with 1 μM forskolin in the presence of M&B28767 at the indicated concentrations, and cAMP levels were determined as described in Materials and Methods. Each point represents the mean ± standard error of two sets of triplicated determinations in COS-7 cells or the mean ± standard error of one set of quadruplicated determinations in CHO cells. The cAMP concentrations in COS-7 cells expressing $EP_{3\text{-IV}}$ and in mock-transfected COS-7 cells without M&B28767 amounted to 23.20 ± 0.26 and 21.05 ± 0.80 pmol/10^5 cells, respectively, and the cAMP concentrations in CHO cells expressing $EP_{3\text{-IV}}$ and in untransfected CHO cells without M&B28767 amounted to 15.76 ± 0.28 and 12.78 ± 0.45 pmol/10^5 cells, respectively. *, Significant decreases in cAMP levels compared with cells expressing $EP_{3\text{-IV}}$ that were stimulated by forskolin alone ($p < 0.05$).

RT-PCR. To further differentiate the five EP_3 isoform mRNA expressions in human tissues, we performed RT-PCR analyses using isoform-specific antisense primers (Fig. 8). RT-PCR analyses revealed the existence of the five EP_3 mRNA species at the expected sizes. The $EP_{3\text{-II}}$ mRNA was detected throughout the tissues examined. The $EP_{3\text{-III}}$ and $EP_{3\text{-IV}}$ mRNAs were also detected in a wide range of human tissues. However, the $EP_{3\text{-III}}$ mRNA was not detected in either the lung or liver, and the $EP_{3\text{-IV}}$ mRNA was not detected in the lung. The $EP_{3\text{-I}}$ mRNA was rather sparsely distributed. One of the two $EP_{3\text{-I}}$ mRNAs (which corresponds to pEPR-Ia) was detected in the brain, renal cortex and medulla, pancreas, uterus, and placenta, whereas the other (corresponding to pEPR-Ib) was detected in the brain, renal cortex and medulla, small intestine, pancreas, aorta, and uterus. On the whole, all the five EP_3 mRNAs were detected in the renal cortex and medulla, pancreas, brain, and uterus. Relatively high expressions of the five EP_3 mRNA species were observed in the kidney, pancreas, and uterus on the basis of β-actin expression in each tissue.

Discussion

In the present study, we succeeded in the isolation of five distinct cDNA clones encoding four different isoforms for human PGE receptor EP_3 subtype. All of the clones contained the common nucleotide sequence from the 5′-untranslated region up to the 1077th guanine nucleotide and the specific nucleotide sequences further downstream in the 3′ portions. Genomic Southern blot analysis with the common nucleotide sequence cDNA probe indicated a single hybridizing band on digestion with various restriction enzymes, demonstrating that these clones are derived from a single gene. These results suggest that the five mRNA species are therefore generated by alternative mRNA splicing. The mouse, bovine, rabbit, and rat EP_3 isoforms are also suggested to be generated by alternative mRNA splicing. Furthermore, Raychowdhury *et al.* (34) recently reported that alternative mRNA splicing produces two different cytoplasmic tails in human thromboxane A_2 receptor. Taken together, these observations suggest that alternative mRNA splicing mechanism is the strategy to generate the variations in the 3′ portions of the prostanoid receptor family.

Based on a comparison of the amino acid sequences in the carboxyl-terminal tails of human EP_3 isoforms with those of mouse, rabbit, and bovine EP_3 isoforms (Fig. 9) (7, 10, 11, 13), human $EP_{3\text{-I}}$ is a counterpart of mouse $EP_{3\alpha}$ and rabbit $EP_{3\text{-}74A}$, human $EP_{3\text{-II}}$ is a counterpart of mouse $EP_{3\gamma}$ and

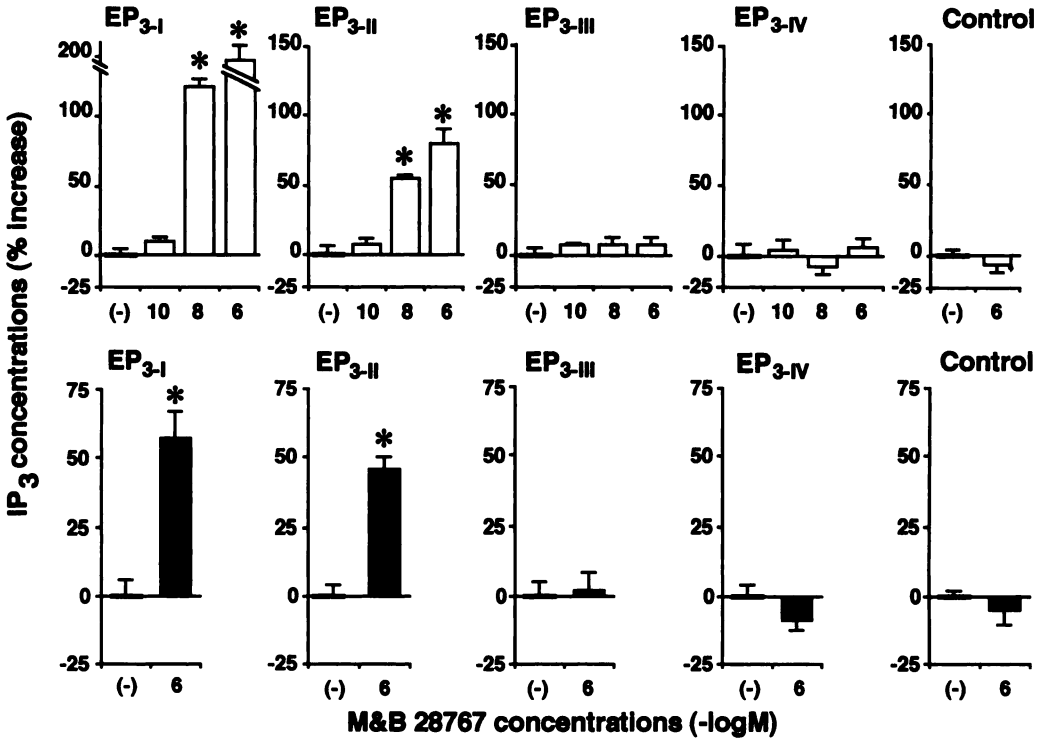

Fig. 6. Comparison of the agonist-induced IP_3 accumulation in COS-7 cells and CHO cells expressing EP_3 isoforms. COS-7 cells (*closed bars*) or CHO cells (*open bars*) expressing EP_3 isoforms, mock-transfected COS-7 cells and untransfected CHO cells were incubated for 30 sec at 37° with M&B28767 at the indicated concentrations. Then, IP_3 levels were measured as described in Materials and Methods. Each concentration represents the mean ± standard error of two sets of triplicated determinations in COS-7 cells or the mean ± standard error of one set of quadruplicated determinations in CHO cells. The IP_3 concentrations in COS-7 cells expressing $EP_{3\text{-I}}$, $EP_{3\text{-II}}$, $EP_{3\text{-III}}$, and $EP_{3\text{-IV}}$ and in mock-transfected COS-7 cells without M&B28767 amounted to 7.40 ± 0.44, 6.00 ± 0.27, 6.80 ± 0.37, 7.80 ± 0.34, and 7.05 ± 0.17 pmol/10^5 cells, respectively, and the IP_3 concentrations in CHO cells expressing $EP_{3\text{-I}}$, $EP_{3\text{-II}}$, $EP_{3\text{-III}}$, and $EP_{3\text{-IV}}$ and in untransfected CHO cells without M&B28767 amounted to 1.95 ± 0.30, 2.26 ± 0.35, 2.18 ± 0.26, 2.08 ± 0.40, and 2.33 ± 0.24 pmol/10^5 cells, respectively. *, Significant increases in IP_3 level in cells expressing the EP_3 isoform ($p < 0.05$).

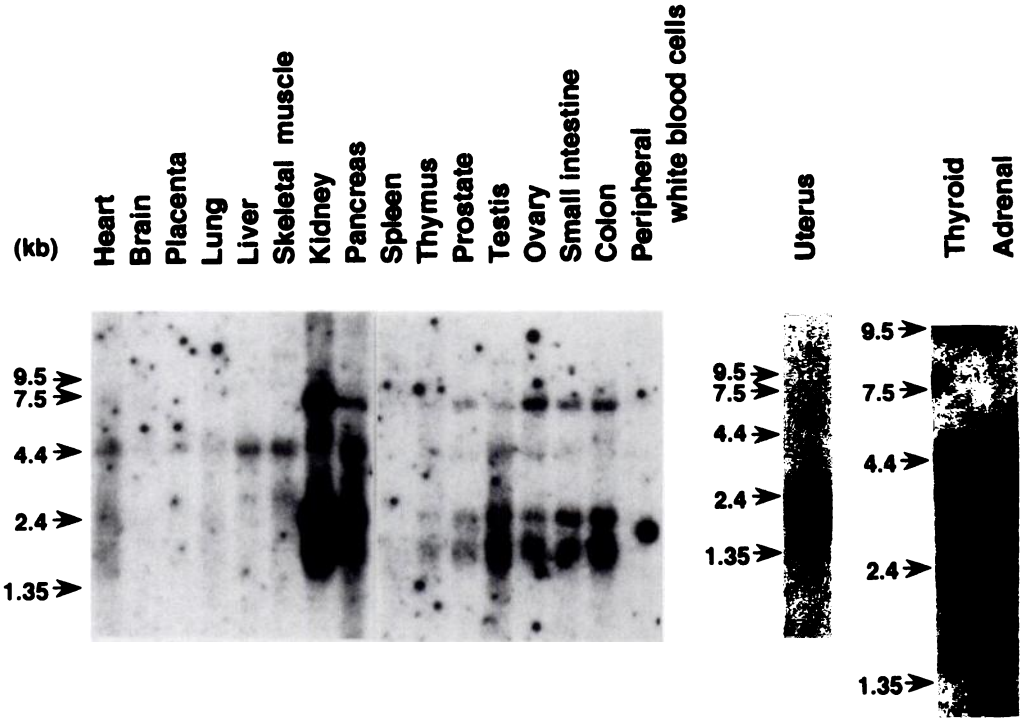

Fig. 7. Northern blot analysis of poly(A)$^+$ RNA (2 μg/lane) from various human tissues. The blots were hybridized with ^{32}P-labeled *Eco*RI/*Bgl*II cDNA fragment of pEPR-Ia. RNA ladders from 0.24 to 9.5 kb in size (GIBCO-BRL) are used as size markers.

bovine EP_{3D}, and human $EP_{3\text{-III}}$ is a counterpart of rabbit $EP_{3\text{-}72A}$. However, human $EP_{3\text{-IV}}$ is a new isoform with a unique carboxyl-terminal tail and an extra 9 amino acid residues in the carboxyl-terminal tail of $EP_{3\text{-III}}$. At present, counterparts of human $EP_{3\text{-IV}}$ have never been reported in any other species. On the other hand, we could not find a

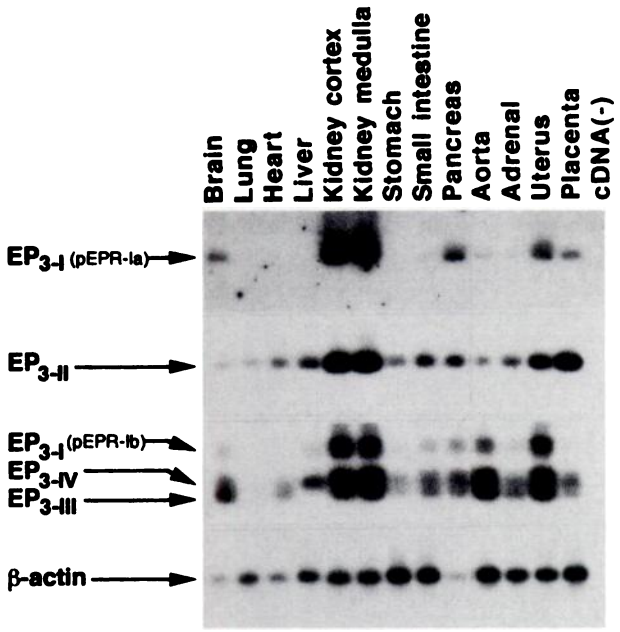

Fig. 8. RT-PCR for EP_3 isoforms and β-actin. RT-PCR analyses for EP_3 isoform-specific mRNAs in various human tissues are shown. Five microliters of the reaction mixture loaded on a 3% agarose gel were transferred onto a nylon membrane and then hybridized with a ^{32}P-labeled internal oligo DNA probe for EP_3 isoforms or a ^{32}P-labeled β-actin genomic DNA fragment as described in Materials and Methods. Each EP_3 isoform-specific amplification product is indicated by an *arrow*. ΦX174 DNA *Hae*III are used as size markers. One typical result is shown from three reproducible results.

human counterpart of mouse $EP_{3\beta}$ in the present study. The cDNA encoding mouse $EP_{3\beta}$ is created by a 89-bp deletion of mouse $EP_{3\alpha}$ cDNA, which is highly homologous with pEPR-Ia (10). However, RT-PCR analysis did not detect a deleted form of pEPR-Ia in any human tissues examined. Variations in EP_3 isoforms may be species specific, but the highly conserved structures of carboxyl-terminal tails among species suggest the presence of other EP_3 isoforms in humans.

During the present study, Adam *et al.* (15) and Regan *et al.* (16) reported the isolation of three EP_3 isoforms that correspond to $EP_{3\text{-I}}$, $EP_{3\text{-II}}$, and $EP_{3\text{-III}}$. In the present study, we isolated two distinct cDNA clones for $EP_{3\text{-I}}$ (pEPR-Ia and pEPR-Ib) with different 3′-untranslated sequences. Regan *et al.* also reported two different cDNA clones for $EP_{3\text{-I}}$. One cDNA clone (EP_{3A}) was identical to pEPR-Ia, but another (EP_{3A1}) was different from pEPR-Ib downstream of the 1196th adenine nucleotide of pEPR-Ib in the 3′-untranslated region (Fig. 1B, *diagonal striped area*). Taken together, these observations indicate that at least three mRNA species encode $EP_{3\text{-I}}$ isoform. As for the cDNA clones for $EP_{3\text{-II}}$ and $EP_{3\text{-III}}$ isolated in the present study, they corresponded to those reported by Adam *et al.* (15).

Previous pharmacological studies have suggested that EP_3 subtype is coupled to at least two different second messenger systems (2). One is the inhibition of adenylate cyclase, and another is the mobilization of intracellular free Ca^{2+}. So far, inhibitory effects of EP_3 isoforms on adenylate cyclase pathway have been reported only in humans (16). In the present study, we demonstrated that EP_3 isoforms are coupled to at least three different second messenger systems, which are the stimulation of cAMP generation and IP_3 generation in addition to the inhibition of cAMP generation. Although human $EP_{3\text{-I}}$ is structurally a counterpart of mouse $EP_{3\alpha}$, human $EP_{3\text{-I}}$ is functionally different from mouse $EP_{3\alpha}$. The former is coupled with two different second messenger systems, the inhibition of adenylate cyclase and stimulation of phosphoinositide turnover, whereas the latter is coupled exclusively with the inhibition of adenylate cyclase via G_i protein and does not stimulate phosphoinositide turnover (10). In contrast, $EP_{3\text{-II}}$ is functionally identical to bovine EP_{3D}, which is shown to be coupled with G_i, G_S, and G_q proteins (7).

Regarding human $EP_{3\text{-III}}$ and $EP_{3\text{-IV}}$, the second messenger systems of these homologues in other species have not been clarified yet. Interestingly, $EP_{3\text{-III}}$ and $EP_{3\text{-IV}}$ are coupled to different second messenger systems, although the structural difference is the deletion or insertion of the 9 amino acid residues in the carboxyl-terminal tails. $EP_{3\text{-III}}$ is reported to be coupled to the inhibition of adenylate cyclase pathway (16). In addition, the present study shows that $EP_{3\text{-III}}$ does not stimulate either cAMP or IP_3 generation. On the other hand, $EP_{3\text{-IV}}$ is capable of both stimulating cAMP generation and inhibiting forskolin-induced cAMP accumulation, whereas its stimulatory effect on IP_3 formation has not been observed. There are some examples showing that G protein-coupled receptors are produced by alternative mRNA splicing. In two isoforms of D_2 dopaminergic receptor, alternative mRNA splicing produces an insertion or deletion of 29 amino acid residues in the third intracellular loop, which does not affect their second messenger systems (35–37). In contrast, five alternatively spliced variants of pituitary adenylyl cyclase-activating polypeptide type-1 receptor have different patterns of adenylate cyclase and phospholipase C stimulation, depending on the different structures in the third intracellular loop (38). We have reported that the carboxyl-terminal tails determine the specificity of coupling with various types of G proteins in bovine EP_3 isoforms (7). Furthermore, the present study demonstrates that the deletion or insertion of the 9 amino acid residues in $EP_{3\text{-III}}$ and $EP_{3\text{-IV}}$ influences, even if not directly, their coupling properties in stimulating adenylate cyclase pathway. These observations reveal that the carboxyl-terminal tails have an important role for the specificity of G protein association and that the alternative mRNA splicing mechanism is able to produce receptor isoforms with different second messenger systems.

Although EP_3 subtype is reported to be present abundantly in the kidney, uterus, and stomach and substantially in the brain, heart, spleen, thymus, lung, and adrenal in mice and rabbits (6, 13), little is known of the detailed distribution of EP_3 subtype in humans. Previous reports showed a restricted distribution of EP_3 in human tissues, i.e., only kidney, pancreas, and small intestine (16). In the present study, Northern blot analysis revealed that five distinct EP_3 mRNA species of 7.5, 5.0, 4.5, 2.5, and 1.9 kb are expressed in a variety of human tissues in a tissue-specific manner. To identify the size of each EP_3 isoform mRNA, we also performed Northern blot analyses with isoform-specific cDNA and/or oligonucleotide probes.[2] The results suggest that the mRNA species of 2.5 and 4.5 kb correspond to pEPR-Ia and pEPR-II transcripts, respectively, and that the mRNA species of 1.8–1.9

[2] M. Kotani, I. Tanaka, Y. Ogawa, T. Ushi, K. Mori, A. Ichikawa, S. Narumiya, T. Yoshimi, K. Nakao, unpublished observations.

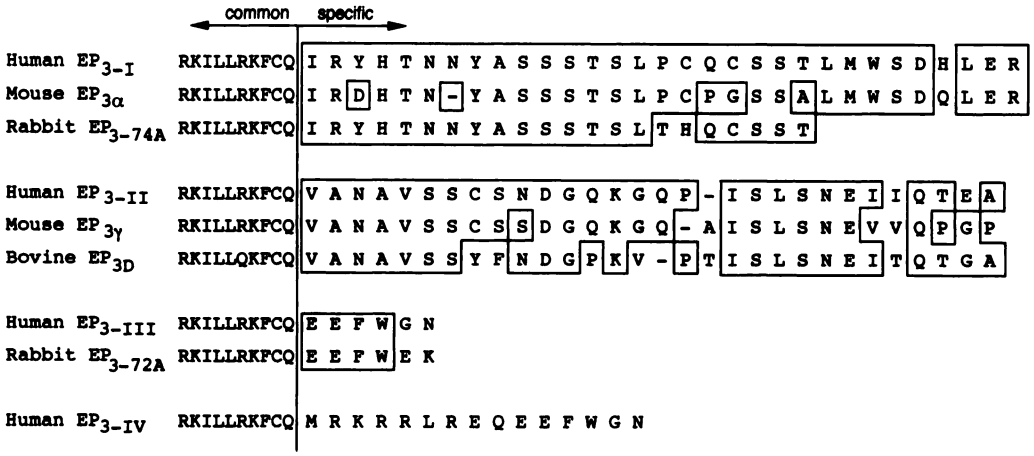

Fig. 9. Comparison of the amino acid sequences of carboxyl-terminal tails of EP_3 isoforms from various species. The deduced amino acid sequences of the carboxyl-terminal tails of the human $EP_{3\text{-I}}$, $EP_{3\text{-II}}$, $EP_{3\text{-III}}$, and $EP_{3\text{-IV}}$; mouse $EP_{3\alpha}$ and $EP_{3\gamma}$; bovine EP_{3D}; and rabbit $EP_{3\text{-}74A}$ and $EP_{3\text{-}72A}$ isoforms are shown. *Boxes*, Identical amino acids. *Bars* indicate gaps introduced in the sequences for maximal alignment.

kb include pEPR-Ib, pEPR-III, and pEPR-IV. However, we could not detect EP_3 mRNA species of 7.5 and 5.0 kb, which may be due to the presence of unidentified isoforms or the low sensitivity of Northern blot analysis using the isoform-specific probes. The precise elucidation of the tissue distribution and size of each isoform mRNA should require the determination of the complete cDNA sequence for each isoform and the EP_3 gene organization. Furthermore, in the present study, RT-PCR analyses using isoform-specific antisense primers revealed tissue-specific distributions of the five EP_3 mRNA species. It is remarkable that multiple EP_3 isoforms coupled to different second messenger systems are present in almost all organs examined. For example, in the small intestine, aorta, and uterus, all of the four isoforms were detected. $EP_{3\text{-I}}$ and $EP_{3\text{-II}}$ might mediate smooth muscle contraction by stimulating IP_3 formations; however, stimulating and/or inhibiting effects of $EP_{3\text{-I}}$, $EP_{3\text{-II}}$, $EP_{3\text{-III}}$, and $EP_{3\text{-IV}}$ on adenylate cyclase may also affect the functions of these organs. These results also suggest that certain effects of PGE_2 on smooth muscle relaxation, which are believed to be mediated by EP_2 and IP receptor (2), may be partially due to $EP_{3\text{-II}}$ or $EP_{3\text{-IV}}$ isoform. Furthermore, in the kidney, EP_3 receptor is reported to inhibit arginine vasopressin-induced water reabsorption by inhibiting adenylate cyclase in renal collecting duct (39). The presence of all of the five EP_3 mRNA species in the kidney led us to speculate that there were multiple functions of PGE_2 and EP_3 isoforms in this organ. *In situ* hybridization revealed that EP_3 mRNA is distributed not only in renal medullary tubules but also in juxtaglomerular apparatus and cortical tubules in mice (40). Further studies are necessary to identify the cell type with EP_3 isoforms and to elucidate their functions in various tissues.

In conclusion, we succeeded in the isolation of five distinct cDNAs encoding four human EP_3 isoforms that are generated by alternative mRNA splicing. The present study will lead to better understanding of multiple functions of PGE_2 in humans and provide further insight into the molecular mechanisms underlying the PGE_2/EP_3 subtype system.

Acknowledgments

The authors thank Dr. Izumi Kotani for her kind encouragements.

References

1. Campbell, W. B. *The Pharmacological Basis of Therapeutics*, 8th ed. (A. G. Gilman, T. W. Rall., A. S. Nies, and P. Taylor, eds.). Pergamon Press, New York, 600–617 (1990).
2. Coleman, R. A., I. Kennedy, P. P. A. Humphrey, K. Bunce, and P. Lumley. *Comprehensive Medical Chemistry*, vol. 3. Pergamon Press, Oxford, 643–714 (1990).
3. Coleman, R. A., S. P. Grix, S. A. Head, J. B. Louttit, A. Mallett, and R. L. G. Sheldrick. A novel inhibitory prostanoid receptor in piglet saphenous vein. *Prostaglandins* **47**:151–168 (1994).
4. Watabe, A., Y. Sugimoto., A. Honda, A. Irie, M. Negishi, S. Narumiya, and A. Ichikawa. Cloning and expression of cDNA for a mouse EP_1 subtype of prostaglandin E receptor. *J. Biol. Chem.* **268**:20175–20178 (1993).
5. Honda, A., Y. Sugimoto, T. Namba, A. Watabe, A. Irie, M. Negishi, S. Narumiya, and A. Ichikawa. Cloning and expression of a cDNA for mouse prostaglandin E receptor EP_2 subtype. *J. Biol. Chem.* **268**:7759–7762 (1993).
6. Sugimoto, Y., T. Namba, A. Honda, Y. Hayashi, M. Negishi, A. Ichikawa, and S. Narumiya. Cloning and expression of a cDNA for mouse prostaglandin E receptor EP_3 subtype. *J. Biol. Chem.* **267**:6463–6466 (1992).
7. Namba, T., Y. Sugimoto, M. Negishi, A. Irie, F. Ushikubi, A. Kakizuka, S. Ito, A. Ichikawa, and S. Narumiya. Alternative splicing of C-terminal tail of prostaglandin E receptor subtype EP_3 determines G-protein specificity. *Nature (Lond.)* **365**:166–170 (1993).
8. Regan, J. W., T. J. Bailey, D. J. Pepperl, K. L. Pierce, A. M. Bogardus, J. E. Donello, C. E. Fairbairn, K. M. Kedzie, D. F. Woodward, and D. W. Gil. Cloning of a novel human prostaglandin receptor with characteristics of the pharmacologically defined EP_2 subtype. *Mol. Pharmacol.* **46**:213–220 (1994).

8a. Nishigaki, N., M. Negishi, A. Honda, Y. Sugimoto, T. Namba, S. Narumiya, and A. Ichikawa. Identification of prostaglandin E receptor 'EP2' cloned from mastocytoma cells as EP4 subtype. *FEBS Lett.* **364**:339–341 (1995).

9. Bastien, L., N. Sawyer, R. Grygorczyk, K. M. Metters, and M. Adam. Cloning, functional expression, and characterization of the human prostaglandin E_2 receptor EP_2 subtype. *J. Biol. Chem.* **269**:11873–11877 (1994).
10. Sugimoto, Y., M. Negishi, Y. Hayashi, T. Namba, A. Honda, A. Watabe, M. Hirata, S. Narumiya, and A. Ichikawa. Two isoforms of the EP_3 receptor with different carboxyl-terminal domains. *J. Biol. Chem.* **268**:2712–2718 (1992).
11. Irie, A., Y. Sugimoto, T. Namba, A. Harazono, A. Honda, A. Watabe, M. Negishi, S. Narumiya, and A. Ichikawa. Third isoform of the prostaglandin-E-receptor EP_3 subtype with different C-terminal tail coupling to both stimulation and inhibition of adenylate cyclase. *Eur. J. Biochem.* **217**:313–318 (1993).
12. Takeuchi, K., T. Abe, N. Takahashi, and K. Abe. Molecular cloning and internal localization of rat prostaglandin E_2 receptor EP_3 subtype. *Biochem. Biophys. Res. Commun.* **194**:885–891 (1993).
13. Breyer, R. M., R. B. Emeson, J. L. Tarng, M. D. Breyer, L. S. Davis, R. M. Abromson, and S. M. Ferrenbach. Alternative splicing generates multiple isoforms of a rabbit prostaglandin E_2 receptor. *J. Biol. Chem.* **269**:6163–6169 (1994).
14. Negishi, M., Y. Sugimoto, A. Irie, S. Narumiya, and A. Ichikawa. Two isoforms of prostaglandin E receptor EP_3 subtype. *J. Biol. Chem.* **268**: 9517–9521 (1993).
15. Adam, M., Y. Boie, T. H. Rushmore, G. Müller, L. Bastien, K. T. Mckee, K. M. Metters, and M. Abramovitz. Cloning and expression of three isoforms of the human EP_3 prostanoid receptor. *FEBS Lett.* **338**:170–174 (1994).
16. Regan, J. W., T. J. Bailey, J. E. Donello, K. L. Pierce, D. J. Pepperl, D. Zhang, K. M. Kedzie, C. E. Fairbairn, A. M. Bogardus, D. F. Woodward, and D.W. Gil. Molecular cloning and expression of human EP_3 receptors: evidence of three variants with differing carboxyl termini. *Br. J. Pharmacol.* **112**:377–385 (1994).
17. Jinhong, Y., X. Menghang, J. G. Edward, and A. Songzhu. Cloning and expression of the EP_3-subtype of human receptors for prostaglandin E_2. *Biochem. Biophys. Res. Commun.* **198**:999–1006 (1994).

18. Kunapuli, S. P., F. M. Guang, M. Bastepe, L. Y. Liu-chen, S. Li, P. P. Cheung, J. K. Deriel, and B. Ashby. Cloning and expression of a prostaglandin E receptor EP_3 subtype from human erythroleukemia cells. *Biochem. J.* **288:**263–267 (1994).
19. Sando, T., T. Usui, I. Tanaka, K. Mori, Y. Sasaki, Y. Fukuda, T. Namba, Y. Sugimoto, A. Ichikawa, S. Narumiya, and K. Nakao. Molecular cloning and expression of rat prostaglandin E receptor EP_2 subtype. *Biochem. Biophys. Res. Commun.* **200:**1329–1333 (1994).
20. Maniatis, T., E. F. Fritsch, and J. Sambrock. *Molecular Cloning: A Laboratory Manual,* 2nd ed. Cold Spring Harbor Laboratory, Cold Spring, New York (1989).
21. Ogawa, Y., H. Itoh, N. Tamura, S. Suga, T. Yoshimasa, T. Serikawa, and K. Nakao. Molecular cloning of the complementary DNA and gene that encode mouse brain natriuretic peptide and generation of transgenic mice that overexpress the brain natriuretic peptide gene. *J. Clin. Invest.* **93:** 1911–1921 (1994).
22. Sussmann, D. J., and G. Milman. Short-term, high-efficiency expression of transfected DNA. *Mol. Cell Biol.* **4:**1641–1643 (1984).
23. Hirth, K. P., Edwards, C. A., and Firtel, R. A.. A DNA-mediated transformation system for *Dictyostelium discoideum. Proc. Natl. Acad. Sci. USA* **79:**7356–7360 (1982).
24. Honma, M., T. Satoh, J. Takezawa and M. Ui. An ultrasensitive method for the simultaneous determination of cyclic AMP and cyclic GMP in small-volume samples from blood and tissue. *Biochem. Med.* **18:**257–273 (1977).
25. Challiss, R. A. J., I. H. Batty, and S. R. Nahorski. Mass measurement of inositol (1,4,5) trisphosphate in rat cerebral cortex slices using a radioreceptor assay: effects of neurotransmitters and depolarization. *Biochem. Biophys. Res. Commun.* **157:**684–691 (1988).
26. Nakajima, S., H. Hamada, P. Reddg, and T. Kakunaga. Molecular structure of the human cytoplasmic β-actin gene: interspecies homology of sequences in the introns. *Proc. Natl. Acad. Sci. USA* **82:**6133–6137 (1985).
27. Kozak, M. The scanning model for translation: an update. *J. Cell Biol.* **108:**229–241 (1989).
28. Kyte, J., and R. F. Doolittle. A simple method for displaying the hydropathic character of a protein. *J. Mol. Biol.* **157:**105–132 (1982).
29. Kennelly, P. J., and E. G. Krebs. Consensus sequences as substrate specificity determinants for protein kinases and protein phosphatases. *J. Biol. Chem.* **266:**15555–15558 (1991).
30. Funk, C. D., L. Furci, G. A. FitzGerald, R. Grygorczyk, C. Rochette, M. A. Bayne, M. Abramovitz, and K. M. Metters. Cloning and expression of a cDNA for the human prostaglandin E receptor EP_1 subtype. *J. Biol. Chem.* **268:**26767–26772 (1993).
31. Nakagawa, O., I. Tanaka, T. Usui, M. Harada, Y. Sasaki, H. Itoh, T. Yoshimasa, T. Namba, S. Narumiya, and K. Nakao. Molecular cloning of human prostacyclin receptor cDNA and its gene expression in the cardiovascular system. *Circulation* **90:**1643–1647 (1994).
32. Hirata, M., Y. Hayashi, F. Ushikubi, Y. Yokota, R. Kageyama, S. Nakanishi, and S. Narumiya. Cloning and expression of cDNA for a human thromboxane A_2 receptor. *Nature (Lond.)* **349:**617–620 (1991).
33. Abramovitz, M., Y. Boie, T. Nguyen, T. H. Rushmore, M. A. Bayne, K. M. Metters, D. M. Slipetz, and R. Grygorczyk. Cloning and expression of a cDNA for the human prostanoid FP receptor. *J. Biol. Chem.* **269:**2632–2636 (1994).
34. Raychowdhury, M. K., M. Yukawa, L. J. Collins, S. H. McGrail, K. C. Kent, and J. A. Ware. Alternative splicing produces a divergent cytoplasmic tail in the human endothelial thromboxane A_2 receptor. *J. Biol. Chem.* **269:** 19256–19261 (1994).
35. Toso, R. D., B. Sommer, M. Ewert, A. Herb, D. B. Pritchett, A. Bach, B. D. Shivers, and P. H. Seeburg. The dopamine D_2 receptor: two molecular forms generated by alternative splicing. *EMBO J.* **8:**4025–4034 (1989).
36. Giros, B., P. Sokoloff, M. P. Martres, J. F. Riou, L. J. Emoline, and J. C. Schwartz. Alternative splicing directs the expression of two D_2 dopamine receptor isoforms. *Nature (Lond.)* **342:**923–926 (1989).
37. Monsma, F. J., Jr., L. D. McVittie, C. R. Gerfen, L. C. Mahan, and D. R. Sibley. Multiple D_2 dopamine receptors produced by alternative RNA splicing. *Nature (Lond.)* **342:**926–929 (1989).
38. Spengler, D., C. Waeber, C. Pantaloni, F. Holsboer, J. Boskaert, P. H. Seeburg, and L. Journot. Differential signal transduction by five splice variants of the PACAP receptor. *Nature (Lond.)* **365:**170–175 (1993).
39. Sonnenburg, W. K., and W. L. Smith. Regulation of cyclic AMP metabolism in rabbit cortical collecting tubule cells by prostaglandins. *J. Biol. Chem.* **263:**6155–6160 (1988).
40. Sugimoto, Y., T. Namba, R. Shigemoto, M. Negishi, A. Ichikawa, and S. Narumiya. Distinct localization of mRNAs for three subtypes of prostaglandin E receptor in kidney. *Am. J. Physiol.* **266:**F823–F828 (1994).

Send reprint requests to: Issei Tanaka, M.D., Ph.D., Second Division, Department of Medicine, Kyoto University, Faculty of Medicine, 54 Shogoin Kawahara-cho, Sakyo-ku, Kyoto 606, Japan.